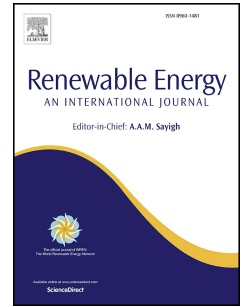


Journal Pre-proof

A real case of thin film PV alternatives to cSi based on a-Si and CdTe. Results after eleven years operating at same conditions

Miguel-Ángel Muñoz-García, Guillermo P. Moreda, M.B. Nieto-Morone, M.C. Alonso-García



PII: S0960-1481(24)02241-9

DOI: <https://doi.org/10.1016/j.renene.2024.122173>

Reference: RENE 122173

To appear in: *Renewable Energy*

Received Date: 20 September 2024

Revised Date: 10 December 2024

Accepted Date: 13 December 2024

Please cite this article as: Muñoz-García M-Á, Moreda GP, Nieto-Morone MB, Alonso-García MC, A real case of thin film PV alternatives to cSi based on a-Si and CdTe. Results after eleven years operating at same conditions, *Renewable Energy*, <https://doi.org/10.1016/j.renene.2024.122173>.

This is a PDF file of an article that has undergone enhancements after acceptance, such as the addition of a cover page and metadata, and formatting for readability, but it is not yet the definitive version of record. This version will undergo additional copyediting, typesetting and review before it is published in its final form, but we are providing this version to give early visibility of the article. Please note that, during the production process, errors may be discovered which could affect the content, and all legal disclaimers that apply to the journal pertain.

© 2024 Published by Elsevier Ltd.

A real case of thin film PV alternatives to cSi based on a-Si and CdTe. Results after eleven years operating at same conditions

Miguel-Ángel Muñoz-García^{1*}†, Guillermo P. Moreda¹, M.B.Nieto-Morone^{1,2}, M.C.Alonso-García²

¹ETSIAAB, LPF-TAGRALIA. Universidad Politécnica de Madrid. Av. Puerta de Hierro, nº 2, 28040 Madrid. España, E-mail: miguelangel.munoz@upm.es

²Departamento de Energía. Unidad de Energía Solar Fotovoltaica. CIEMAT. Av. Complutense, 40, 28040, Madrid, España.

The new PV technologies need to be analysed in the long term to obtain mature results. Technologies such as tandem amorphous silicon and Cadmium Telluride were installed in the same conditions ten years ago. Now, the results of their operation are presented with the aim to offer real data to the market

KEY WORDS: Cadmium Telluride, Cd-Te, Amorphous Silicon, a-Si, degradation rate, half-lifetime

1. Introduction

1.1. Photovoltaics expansion worldwide

The climate crisis caused by global warming due to the continuous and growing CO₂ emissions since the beginning of the massive consumption of fossil fuels, has led to the general consensus that the solution lies in massive use of energies that do not emit CO₂ and that emit the least possible amount of greenhouse effect gases in their life cycle.

Among the technologies for electrical power generation, one of the most promising is photovoltaics, since it is easy to install, maintain and increasingly efficient. It should be noted in this last point that efficiency is not only relative to the amount of energy converted, but to be able to compare with other energy sources like wind power or fossil fuels, the associated impacts and consequences must be considered. In this sense, photovoltaics is not only efficient but also safe and cost-effective.

The photovoltaic installed capacity in Spain has grown from 4.6 GW and 8.3 GWh in 2013 (start date of this study) to 25.5 GW and 37.3 GWh in 2023 (REE, 2024).

1.2. Mature and emerging photovoltaic technologies

The increase in the use of photovoltaic energy has led to greater investment in research that has led in turn to an improvement in the efficiency of solar panels. In the last 10 years, efficiency has risen from 16% for crystalline silicon panels in commercial use, to the current 22% (Fraunhofer ISE, 2024). These data are surpassed in the laboratory, with an efficiency of 24.7% for the best performing crystalline silicon panels (Fraunhofer ISE, 2024), and foreseeably will be transferred to the public.

All PV technologies have undergone an increase in efficiency supported by research. Almost all of them do not only owe this increase to improvements in manufacturing but

* Correspondence to: Miguel-Ángel Muñoz-García, Universidad Politécnica de Madrid.

Dep. Ing. Agroforestal-Electrotecnia y Energías Renovables. LPF-TAGRALIA.

Avda. Complutense s/n, 28040 Madrid, Spain

† E-mail: miguelangel.munoz@upm.es

also to the incorporation of mixed technologies, which make it difficult to classify, for example, amorphous silicon as such, since it usually includes layers of microcrystalline silicon. In any case, other materials such as cadmium telluride have clearly improved in efficiency, going from 9% to nearly 20% in the last 10 years (Fraunhofer ISE, 2024). In contrast, efficiency increase for hydrogenated amorphous silicon a-Si:H has been rather smaller, from 9.5% in 2004 to 10.3% in 2015 (Stuckelberger et al., 2017).

Notwithstanding the large efficiency increase of CdTe, most new commercial PV plants worldwide are equipped with crystalline silicon panels. The main reason is that crystalline silicon average annual degradation rate, measured as percent maximum power loss per year, is lower and more predictable. Piliouguine et al. (2022) compiled the degradation rates reported in scientific literature from 2001 to 2021 for thin film PV technologies, and for CdTe, values show a high dispersion, from 0.53% to 10.60%. Contrarily, the certainty on crystalline silicon degradation rate is higher; as a rule of thumb annual degradation rate is below 0.50%. For instance, Pascual et al. (2021) measured an average annual degradation rate of 0.27% for the non-defective panels in a commercial population of 82 MWp panels over 10 years, where the non-defective panels represented about 80% of the total panels population.

2. Objectives of the work

The objective of this work is to present, analyse and discuss the operational evolution of three experimental photovoltaic systems, operating in the same environmental conditions, which were installed for experimentation in 2012 and therefore would have reached half of their theoretical useful life.

The objectives can be summarized as:

- What is the degradation rate for each technology?
- What electrical parameters are more affected by aging?
- What is expected from emerging technologies such as CdTe with the new advances?

This study will help to understand how solar plants in operation with the same technology, installed in the same period, are behaving and whether they may present deficiencies or not, according to what the conclusions of the experiment will provide. Although this is not a large-scale experiment, the results are significant enough considering the controlled conditions and the different technologies working under the same conditions.

3. Materials and Methods.

3.1. The experimental solar plant

The PV plant referred herein is a grid-connected flat-roof PV plant located in one of the buildings of the School of Agricultural Engineers (ETSIAAB) in Madrid, Spain (40.4426 °N, 3.7295 °W). The use of photovoltaic installations on roofs of public buildings has an additional educational function, especially when the buildings host universities.

At the installation date (2012) of the plant used in our research, educational photovoltaic installations were hardly common in Spain, limited to research functions.

The plant used fulfils two objectives: on the one hand, it is used to investigate a comparison of different photovoltaic module technologies and on the other hand, it has been carrying out dissemination work on photovoltaic technologies applied to the agricultural field.

95
96 Since it is a grid-connected plant, with discharge for sale at a fixed price (Ministerium of
97 Industry of Spain, 2008), the electricity is used both energetically, being used in the
98 buildings themselves as they are the closest consumer, and economically, due to the return
99 for the sale of the energy produced.

100
101 According to the legislation in force at the time of installation, the plant, because it has a
102 power of 18.6 kWn and therefore less than 100 kWn, is considered small in size and
103 susceptible to selling energy at a better price. The entire plant is connected to the electrical
104 grid, however, monitoring is closer on the 3.6 kWn experimental part.

105
106 The study consists of comparing common multicrystalline silicon photovoltaic generators,
107 amorphous silicon photovoltaics and cadmium telluride photovoltaics. Each technology is
108 connected to an independent inverter although the three inverters are of the same power and
109 model and the input voltage is similar for the three. This allows detailed data for each section
110 to be recorded for later analysis.

111
112 The project involves not only professors and researchers from both the UPM and institutions
113 such as CIEMAT, but also students who collaborate in different tasks and whose
114 participation contributes to a better understanding of the technology and its dissemination
115 in an area with many possibilities for photovoltaic applications.

116
117 The installation was designed in collaboration with CIEMAT Photovoltaic Solar Unit, with
118 the purpose of measuring the real outdoor performance of relatively new technologies.

119
120 The system is divided in two main sections, A and B (Figure 1). Section A is the largest
121 and it is devoted to electricity production, although it is monitored as well, and the data are
122 registered by a computer program. Section A is formed by two sub-sections, A1 and A2,
123 with the following features:

- 124
- 125 • A1: 45 SUNTECH POWER STP 280 24 Vd panels distributed in three series of 15
126 panels each, connected to the MPPT1 of an SMA STP15000TL three-phase inverter
127 (Inverter No. 1).
- 128 • A2: 18 Polysol 235 DS IBC panels in a single series connected to the MPPT2 of the
129 same inverter as sub-section A1 (Inverter No. 1).

130 Section A is in total $12600 + 4230 = 16830$ Wp, or 15 kWn.

131
132 Section B, namely the research-focused section, is subdivided in three sub-sections, B1, B2,
133 and B3, with the following characteristics:

- 134
- 135 • B1: 7 SUNTECH POWER STP230/20Wd panels in a single series connected to
136 SB1200 inverter (Inverter No. 2): 1610 Wp or 1200 Wn.
- 137 • B2: 16 SCHOTT SOLAR ASI 105DG panels forming two series of 8 panels
138 connected to SB1200 inverter (Inverter No. 3): 1680 Wp or 1200 Wn.
- 139 • B3: 20 FIRST SOLAR FS 382 panels forming four series of 5 panels connected to
140 SB1200 inverter (Inverter No. 4): 1650 Wp or 1200 Wn.



Figure 1 Google Maps view of the PV plant.

142
143

144 While subsection B1 panels are of multicrystalline silicon, subsection B2 panels are of a-Si
145 and subsection B3 are of CdTe. With regard to B2 panels, they are made of homojunction
146 a-Si:H/a-Si:H tandem cells, with the manufacturer code letters DG standing for double glass
147 i.e. front and back glass (Stuckelberger et al., 2017).

148

149 The three sub-sections sum a total of 4.94 kWp or 3.6 kWn.

150

151 The tilt-angle of the panels is 30° and their orientation or Azimuth angle is 2° SE. The
152 supporting structure consists of Aluminium profiles, ballasted with concrete slabs. The
153 whole plant reaches 21770 Wp or 18600 Wn. Each section and subsection is monitored
154 using a computer based program connected to the inverters of every section so that a
155 comparative analysis can be performed.

156

157 3.2. Analysis methodology

158

159 A combination of laboratory tests and actual operation data collection under the same
160 conditions is used for the analysis. In the first case, sampling was carried out measuring
161 four panels of Crystalline Silicon (c-Si) and Amorphous Silicon (a-Si) over 10 years in
162 2012, 2015 and 2023. Likewise, for the Cadmium Telluride technology (CdTe) tests were
163 conducted in 2012 and 2023, by measuring four panels of this technology.

164 Of the four panels of each technology tested, three were temporally dismantled off the PV
165 plant (section B) and transferred to CIEMAT for subsequent measuring. For each
166 technology, the fourth panel tested, or reference panel, was not installed at the plant, i.e. the
167 three reference panels were not in operation. Instead, these three panels had been kept in
168 the dark from year 2012, and they were transferred to CIEMAT together with their outdoor

169 or in-operation counterparts. In this way, it is possible to detect possible fluctuations either
 170 in the measuring equipment that, due to the time that has elapsed, has required changes, or
 171 in possible variations in the method due to changes in the operators involved. In the case of
 172 the CdTe panels, an activation was also carried out due to the accumulation of radiation
 173 prior to the measurements.

174
 175 Indoors measurements were obtained using a flash pulsed class AAA IEC 60904-9 [(IEC
 176 2007)] solar simulator (10 ms pulse). An I-V curve measurement was performed
 177 according to IEC 60904-1 [(IEC 2008)], which obtained the main parameters, I_{sc} , V_{oc} ,
 178 I_m , V_m P_m and FF at Standard Test Conditions (STC):

- 179 - Irradiance: 1000 W/m²
- 180 - Cell temperature: 25°C
- 181 - Spectral distribution: AM1.5G (according to IEC 60904-3)[(IEC 2008)].
- 182 - Normal incidence

183
 184 Temperature of the modules was obtained using a Fluke® thermometer with dual
 185 thermocouple input and sensors connected on representative separated points of the module
 186 to obtain the mean value.

187 Inside the simulator, conditions were very close to STC with little deviation (25 ± 2 °C and
 188 1000 ± 5 W/m²). Using module temperature coefficients (α , β) and irradiance correction
 189 factors, the obtained measurements were extrapolated to STC (see IEC 60891 Standard).
 190 Special care was taken in ensuring that PV modules had not received direct solar light before
 191 the first round of measurements.

192 193 194 3.3. The stabilization issue for aSi and activation process for CdTe

195 The measurement of photovoltaic panels of thin film technologies is not a totally obvious
 196 matter. For example, the output power of an a-Si panel depends on panel history of sunlight
 197 exposure and on recent hours of sun radiation (Mateo et al., 2018). In general, thin film are
 198 materials with less maturity than crystalline silicon and often undergo changes not only
 199 between manufacturers but within the same producer and even within the same model,
 200 depending on the manufacturing batch.

201
 202 As for amorphous silicon, technology has evolved from single junction panels to other
 203 devices in which microcrystalline silicon is stacked into double junction technologies. In
 204 our case, the panel technology is a-Si:H/a-Si:H tandem cells. These panels stabilize in the
 205 first weeks of life, losing up to 20% of their initial power. After such a process, the power
 206 loss is usually less than in crystalline silicon. In addition, it has an "annealing" process
 207 during the days with the highest radiation that produces an effect of improving efficiency
 208 compared to winter days. In addition, the spectral response must be taken into account, since
 209 the simulators are usually calibrated for crystalline silicon cells and panels. Taking all these
 210 aspects into account, the measurements can be extrapolated to be compared between years
 211 and between technologies.

212 213 214 3.4. Experiments setup and test samples used

215 The comparison has been made from two points of view. First, real power and energy were
 216 compared along the years. Such data are in fact of great interest for owners, worried by their
 217 investment and payback time. But must be put besides laboratory data in order to obtain
 218 significant conclusions.

219 In this way, long term continuous data were obtained from the internal dc-ac converters
220 whose data were sent to a logger and compiled periodically for the analysis.

221

222 3.5. Visual inspection

223 Throughout the more than ten years in operation of the plant, no complete failures have
224 been detected in the panels of any of the technologies. However, the gradual drop in power,
225 which may be a normal effect due to degradation within the usual range, may be associated
226 with failures that can be detected with the unaided eye. For this reason, a visual inspection
227 is also carried out to detect defects such as delamination, yellowing or breaks in both the
228 frame and the glass.

229 The process for the visual inspection, follow IEC recommendations (61215, 61646), and
230 should be performed under the following conditions:

- 231 • 1000 lux
- 232 • Unaided eye

233 It must be documented by taking photographs and it is valid for the detection of:

- 234 • Bubbles, delamination, yellowing, browning
- 235 • Broken or split cells, discoloration
- 236 • Burnt or oxidized metallization
- 237 • Peeling, misaligned, scratched or broken frame
- 238 • Delamination or bubbles on the back side
- 239 • Peeling oxidation or corrosion of the connection box
- 240 • Wiring problems: disconnection, loose parts

241

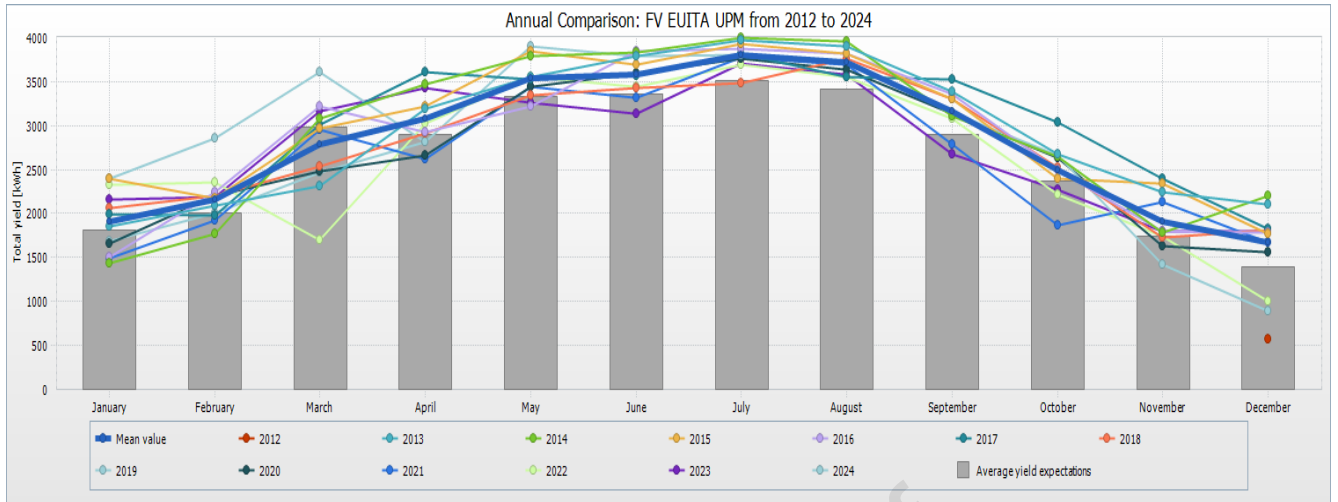
242 4. Results and discussion

243 Three different photovoltaic technologies working in the same real conditions were analysed
244 along ten years of operation. Throughout these years, the insulation of the roof had to be
245 changed during the spring of 2019, something that was barely noticed in production during the
246 month of March 2019. In addition, it suffered the heaviest snowfall in Madrid in more than a
247 century during the winter of 2020 (Muñoz-García et al., 2021) and once again the plant
248 withstood this event well.

249 4.1. Actual production results and plant performance

250 Despite the degradation of the panels expected over the years, the plant has been producing
251 electricity above expectations, possibly due to a good Performance Ratio (PR) given the
252 special care taken in its design. Even so, the gradual drop in production can be seen in Figure
253 2, Figure 3 and Figure 4 being within the expected margins. This graph represents the total
254 production of the plant, which is mainly due to crystalline silicon panels (subsections A1,
255 12600 Wp, A2, 4230 Wp, and B1, 1610 Wp, or 18440 Wp out of the plant total 21770 Wp)

256

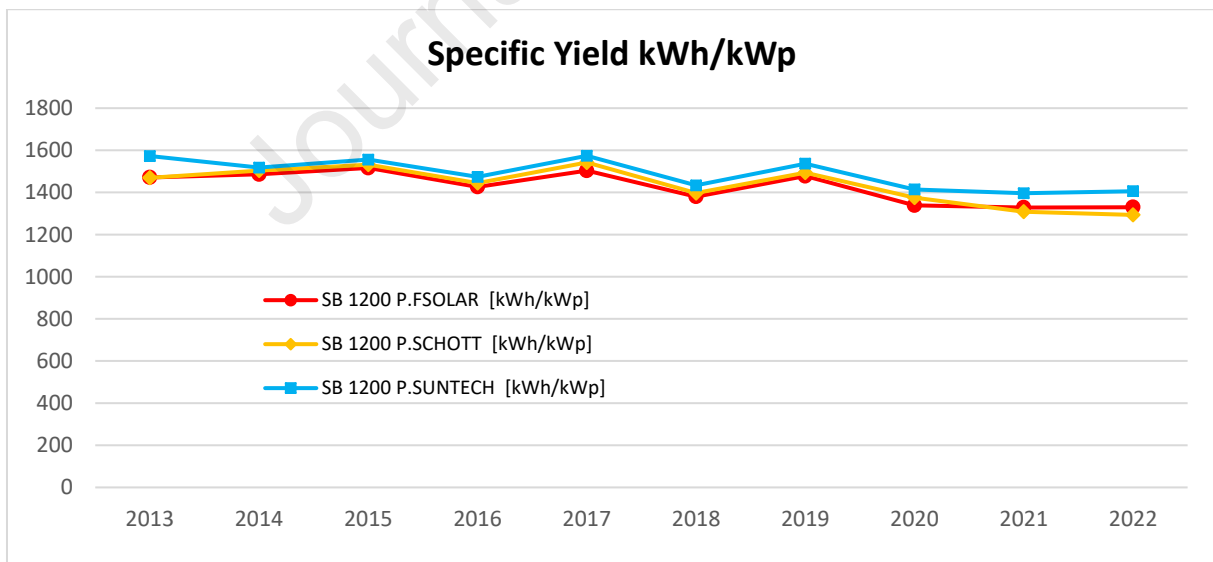


257
258
259

Figure 2.- Monthly comparison of the real and predicted production for the whole plant (PSH expected: 1600).

260
261
262
263
264
265
266
267
268
269
270

When we analyse the different areas of the solar plant, using the real data, we obtain interesting results. In general, production decreases with the course of time, but according to the expected due to the degradation effect. We must consider also the specificities of each year. In 2023 the CdTe area had less modules due to maintenance reasons, so it should be excluded from the comparison. Nevertheless, that year was also hotter than usual what could affect to a better performance of the aSi modules, due to thermal annealing (Hamelmann et al., 2016; Wang et al., 2017).

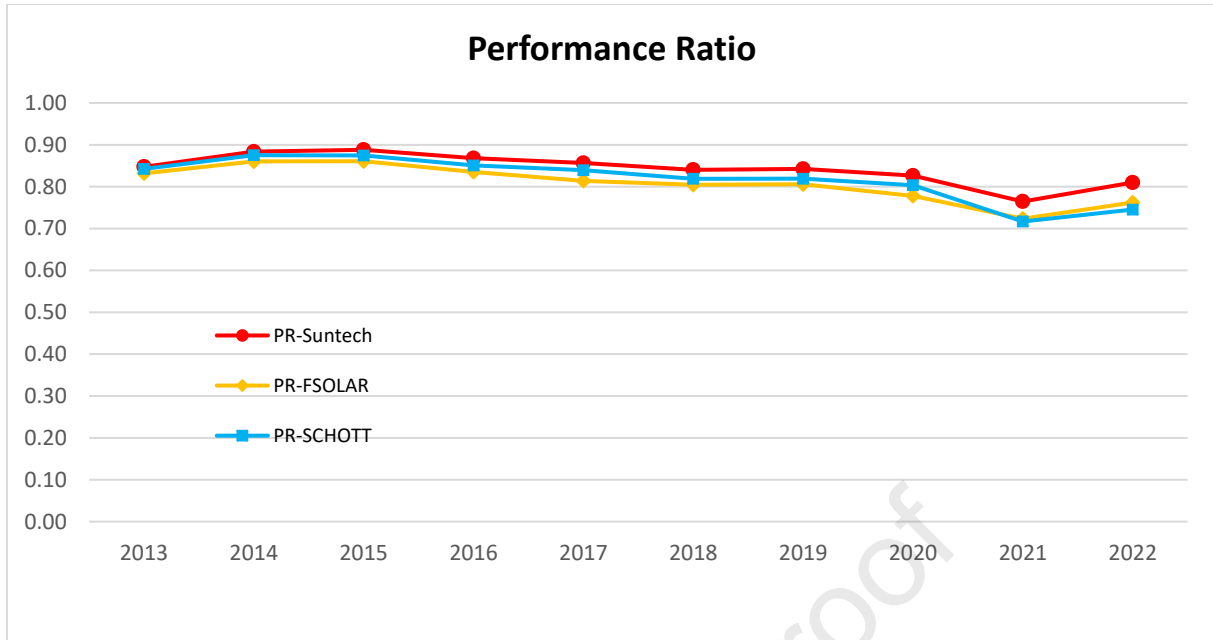


271
272

Figure 3.- Specific yield for each technology along the analysed period.

273
274
275
276
277
278

The PR calculated and shown in Figure 4 carried out considering the yield of generated energy, the peak power of each section and the peak solar hours. No correction is made for temperature, so that the variability of the different technologies can be appreciated in their real form.



279
280
281

Figure 4.- Performance Ratio (PR) calculated for each technology section.

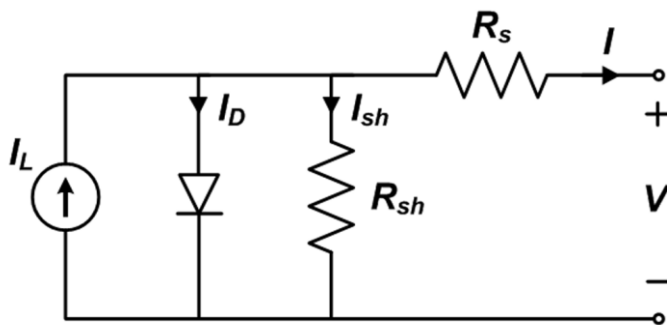
282
283
284

4.2. Indoor flash solar simulator for I-V measurement of I-V characteristic curve.

285 The I-V curve of a PV module is the standard measurement to evaluate its performance in
286 all its operation range at certain irradiance, temperature and spectrum conditions. Measured at
287 Standard Test conditions (irradiance of 1000 W/m², 25°C of module temperature and reference
288 spectrum AM 1.5G), it permits to make comparisons among different module types, or to
289 evaluate the long-term evolution of the same module trough periodical measurements. The
290 current voltage characteristic of a PV module can be described by Equation 1, (Wolf and
291 Rauschenbach, 1963), which corresponds to the electrical circuit of Figure 5 .

$$I = I_L - I_0 \left[\exp\left(\frac{V + IR_s}{mV_t}\right) - 1 \right] - \frac{V + IR_s}{R_{sh}} \quad \text{Equation 1 .- Electrical model for a PV cell}$$

292
293



294
295
296 Figure 5.- Electrical circuit corresponding to equation 1. I_D is the current trough diode due to recombination, developed in equation 1 according to Wolf and Rauscehnbach 1963.

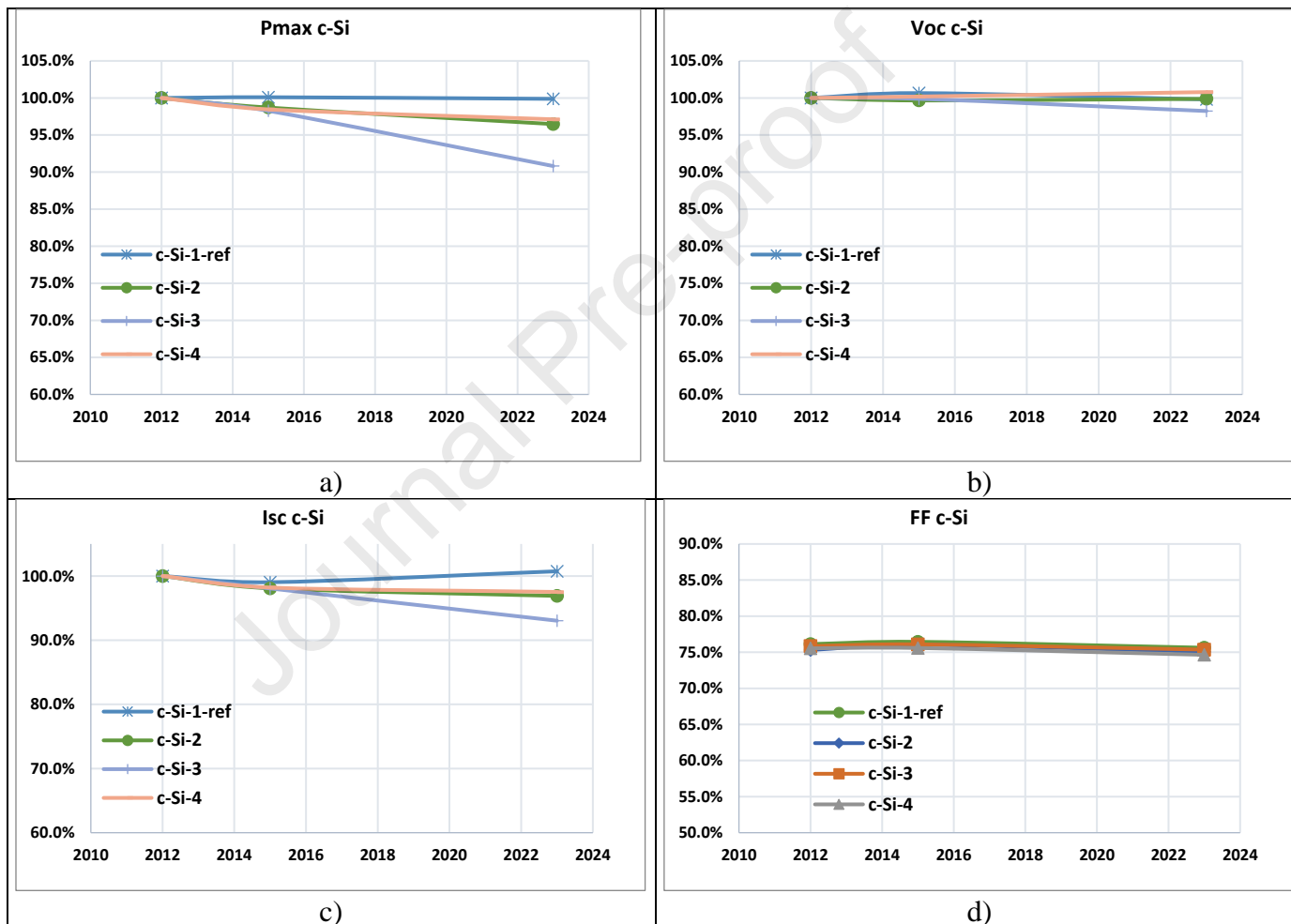
297
298 In Figure 5 the I_D is the current trough diode due to recombination, developed in Equation 1
299 according to Wolf and Rauschenbach 1963. Both Equation 1 and Figure 5, include the
300 following parameters: I_L as the photogenerated current, I_0 the diode saturation current, m de
301 diode ideality factor, V_t the thermal voltage (kT/e), R_s the series resistance and R_{sh} the

302 resistance. Variation in circuit parameters, such as R_s and R_{sh} , due to aging, can be reflected
 303 in I-V curve characteristic parameters as short circuit current (I_{sc}), open circuit voltage (V_{oc}),
 304 maximum power current (P_{max}) and fill factor ($FF = P_{max}/I_{sc} \times V_{oc}$).

305
 306

307 Despite the degradation of the panels expected over the years, the plant has been working
 308 according to expected. This section presents the results of the performance of crystalline c-Si,
 309 amorphous a-Si and cadmium telluride CdTe PV modules compared over the years 2012, 2015
 310 and 2023. In the following figures, the parameters maximum power, open circuit voltage, short
 311 circuit current and fill factor are shown. These measurements were taken under STC following
 312 IEC 61215 standards.(International Electrotechnical Commission, 2005)

313
 314

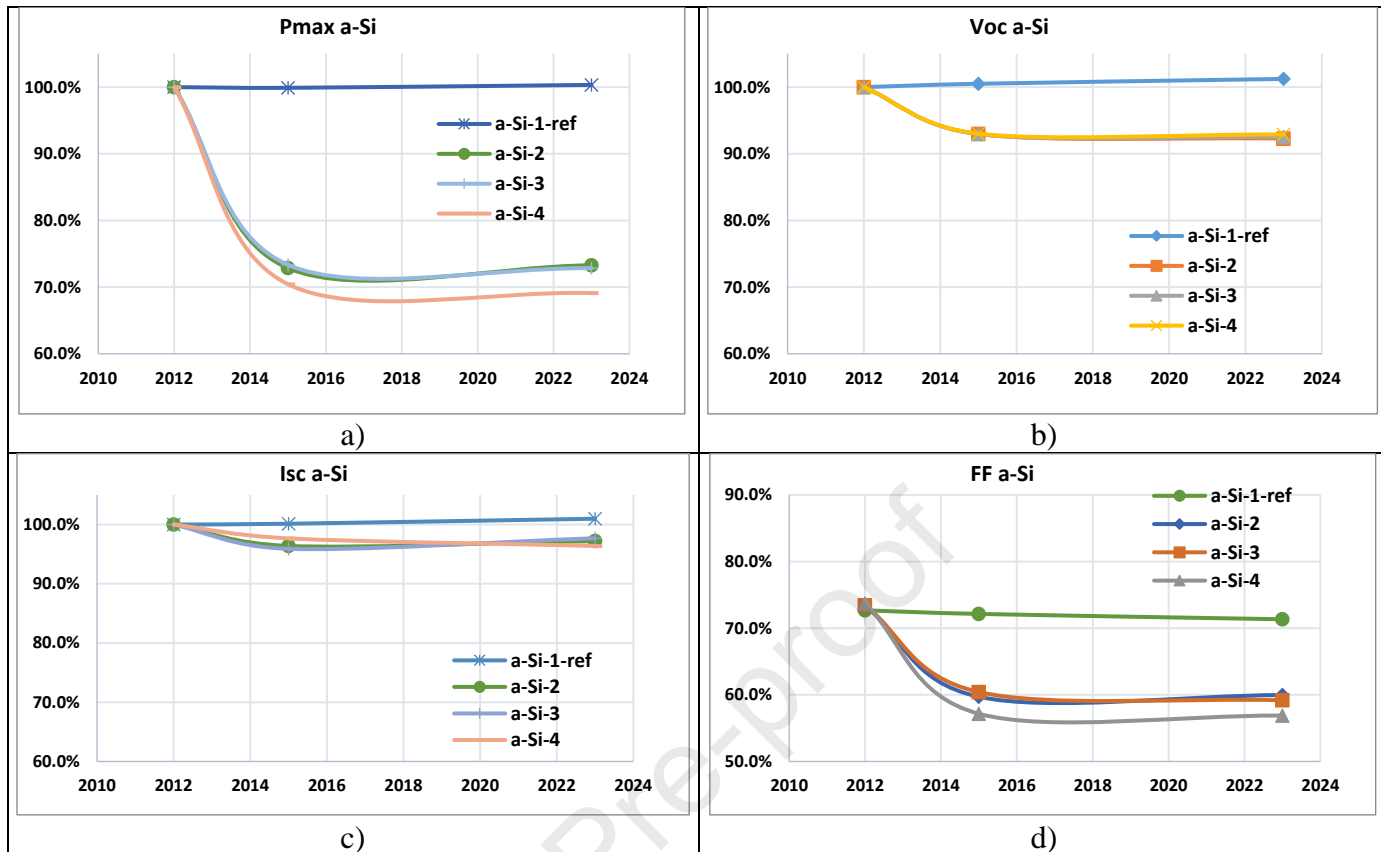


315 Figure 6.- Parameters evolution along ten years for cSi, including reference module and three in-operation modules. a)
 316 maximum power, b) voltage in open circuit, c) short-circuit current and d) fill factor.

317 These group of modules demonstrated a stable performance over the period of study with a
 318 slight decline in Pmax and FF. The values for Pmax declined from 3% (modules 2 and 4) to
 319 10% (module 3), while the reference module remained stable without losses.

320 The open circuit voltage presented a lower descent (1-2%) compared to the short-circuit current
 321 (3-7%), thus indicating the robustness of this technology under sustained operational
 322 conditions.

323
 324



325 Figure 7.- Parameters evolution along ten years for aSi, including reference module and three in-operation modules. a)
 326 maximum power, b) voltage in open circuit, c) short-circuit current, and d) fill factor.

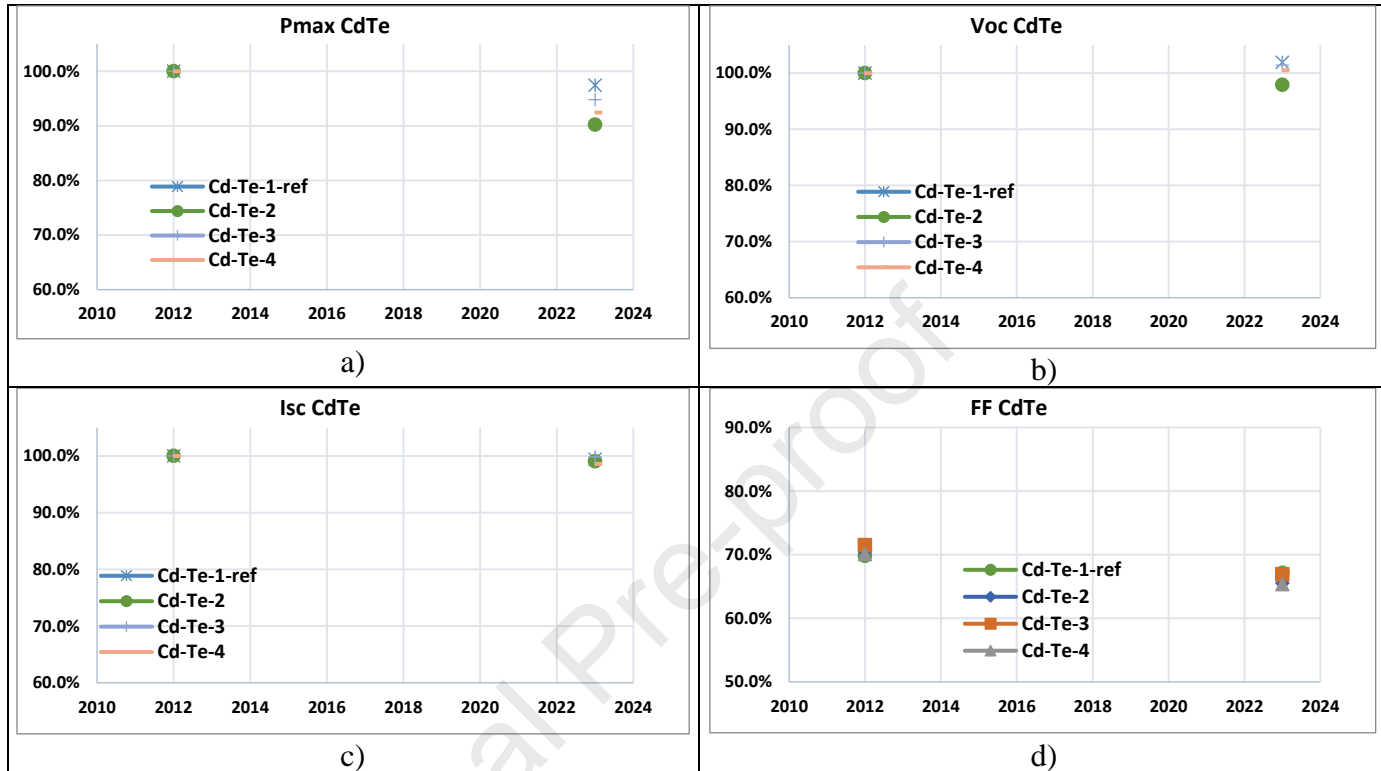
327 The analysis of the a-Si modules is of great interest. Unlike crystalline silicon, in which initial
 328 power stabilization ends after the first few days of panel outdoor exposure (Munoz et al., 2011),
 329 a-Si takes longer to stabilize, typically they do after 1000 hours of light exposure (Berov et al.,
 330 2014). Amorphous silicon technologies suffer from an initial light induced degradation known
 331 as Staebler–Wronski effect (Staebler and Wronski CR, 1977). The stabilization period depends
 332 on the type of module and the environmental conditions, with documented periods of
 333 stabilization from 6 weeks to one or more years (Piliouguine et al, 2022 b). In our case, this
 334 stabilization seems to be achieved after one year and half, and it is observed in all module
 335 parameters, Isc, Voc, Pmax and FF.

336 Thereby, an aspect of utmost importance regarding improvement of a-Si application is
 337 stabilized conversion efficiency (Ichikawa et al., 1990). In our case, it can be seen how after
 338 the initial stabilization, where the panels lose more than 27% (an effect that is known and does
 339 not imply irreversible degradation but, as mentioned, stabilization), the electrical parameters
 340 remain stable over time with a non-significant degradation of Pmax, Isc and Voc. Even the fill
 341 factor remains stable from the second measurement (2015) to the last one (2023). Piliouguine et
 342 al. (2022b) found that while in the first two years of operation the degradation of a-Si panels is
 343 mainly due to a decrease of the current, the long-term degradation is dominated by the reduction
 344 in voltage. Nakamura et al. (2023) reported an annual degradation rate of 3.776% for the first
 345 two years of operation of their a-Si panels followed by 0.31% per year in the eight next years.

346 Among the reasons to explain degradation and failure modes in amorphous silicon, they are
 347 mentioned at the cell level the diffusion of dopants and impurities causing loss in FF, Isc and
 348 Voc, other element diffusion or corrosion causing changes in parasitic resistances (both, Rs and
 349 Rsh, abovementioned on Equation 1), or lamination stresses (the separation of the encapsulating

350 layer, which can modify the optical conditions) causing I_{sc} decrease (McMahon 2004, Radue
 351 2010). At the module level it is observed interconnect or busbar degradation causing changes
 352 in electrical resistances, solder joint degradation or encapsulation failures, provoking loss in
 353 fill factor and I_{sc} . (McMahon 2004, Radue 2010).

354



355

356 *Figure 8.- Parameters evolution along ten years for CdTe, including reference module and three in-operation modules. a)*
 357 *maximum power, b) voltage in open circuit, c) short circuit current and d) fill factor.*

358 Regarding CdTe modules, they showed a different degradation pattern compared to the two
 359 groups of panels analysed above. Although P_{max} output values decreased a 9,8 %, open circuit
 360 voltage and short-circuit current remain reasonably stable. Thus, the degradation came from the
 361 descent in the fill factor, which points at the degradation of internal parallel and series
 362 resistances. Nevertheless, the degradation rate remained within the expected values.

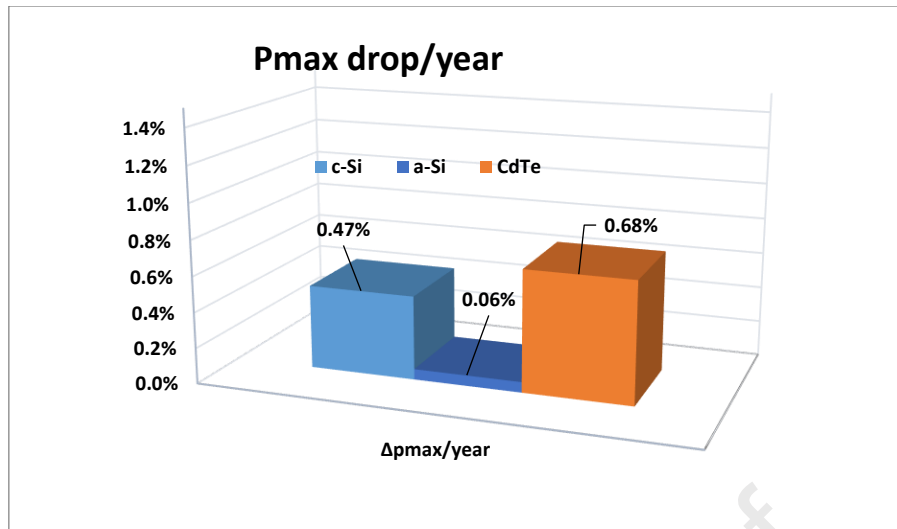
363

364 4.2.1. Comparison of power drop between technologies

365

366 We have a very significant image of this analysis in the comparison of the power variation of
 367 the different technologies. We can see in Figure 9 that, as above-mentioned, the test found that
 368 none of the modules tested had a power drop greater than expected. Likewise, the reference
 369 panel (which in all cases presented stable behaviour) has been excluded from the graph, and an
 370 average of the annual power drop has been obtained for each of the technologies.

371



372
373 *Figure 9.- Comparison of the annual power drop for the three technologies.*

374

375 It can be seen how the one that presents the best performance is the a-Si, although its efficiency
376 is the lowest, so the use of space must be considered. But even so, its performance has been
377 very good with a non-significant power drop (less than 0.1%). It should be noted that the effect
378 of annealing may have an influence on these measurements, but even so, the behaviour is proven
379 to be very good.

380 On the other hand, we have classic silicon, whose behaviour is also stable, and the power drop
381 is less than 0.5% per year, within expectations.

382 Finally, CdTe technology remains promising. Since we must consider that the modules analysed
383 were manufactured more than eleven years ago and during this time improvements have
384 continued to be produced. In the case of CdTe, the power drop is less than 1% per year, being
385 fundamentally due to the worsening of the fill-factor.

386

387

388

389 4.3. Visual defects detected

390 After more than ten years in operation, none of the solar panels seems to suffer important
391 damages. Although degradation of parts such as glass can be detected in certain areas, in one
392 case it can lead to a possible failure over time. The panel with said possible failure is not one
393 of those included in the indoor analysis. Nor is a significant drop in power or voltage detected
394 in the string in which said panel is connected.

395

396 On the other hand, cSi panels present generalized yellowing. Once again, this is a visual defect
397 that, in view of the results of the energy generated as well as the data obtained in the solar
398 simulator, does not seriously affect operation.

399

400 The Figure 10 shows a general view of the cSi experimental area. A yellowing effect is clearly
401 observed in the image. This effect is not present in the panels that are part of the non-
402 experimental area. The difference between one area and another is the aspect orientation of the
403 panels, since they are the same brand and model. This could lead to thinking about an effect of
404 greater heat accumulation in panels that are placed vertically (portrait aspect) as a possible cause
405 of the difference, since the ambient temperature and radiation is the same in both cases.

406

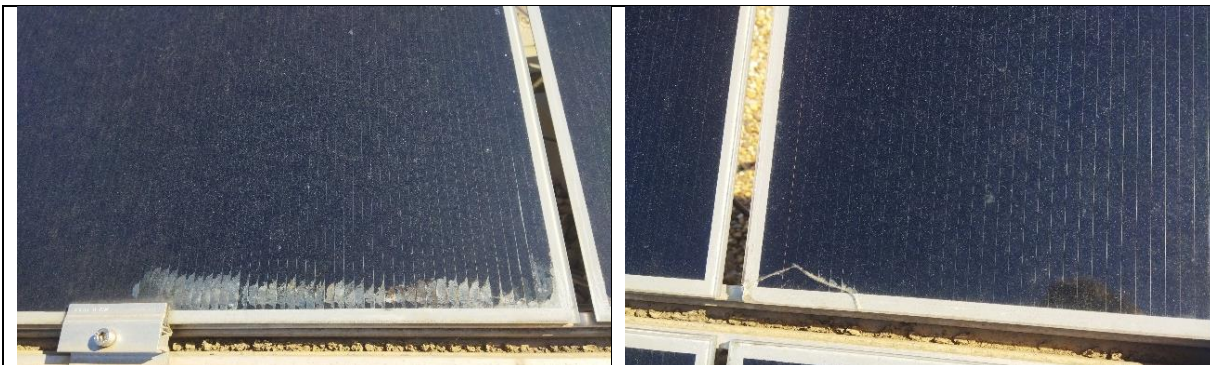
407 As mentioned above, the performance of the PV plant in general and the crystalline silicon
408 panels in particular was within or even surpassed expectations during the first eleven years.

409 Nevertheless, these expectations are based on uncooled PV panels. Undoubtedly, cooling
 410 crystalline silicon panels would enhance their electrical conversion efficiency, since cooling
 411 counteracts the temperature coefficient issue of silicon crystalline technology, generally
 412 quantified as a 0.45% decrease in efficiency for every 1 °C rise of solar cell temperature above
 413 25 °C (Cavadini & Cook, 2021). A variety of PV panel cooling systems have been tested in the
 414 last decades. (Dida et al. 2021) attached a wet burlap cloth to the rear surface of an 80 Wp
 415 multicrystalline silicon panel. The evaporative cooling of the water absorbed by the cloth led
 416 to a temperature decrease of 17 °C compared to the reference PV panel. This translated into an
 417 electrical efficiency increase that ranged between 9% and 14.8% throughout the day. The
 418 average water consumption of their 80 Wp panel was 0.39 L·h⁻¹. Another possibility to cool PV
 419 panels is trickling water on the front surface of the panel. This method has the merit that the
 420 trickled water not only cools the PV panel, but also washes it. A synergistic PV panel cooling
 421 approach is the so-called hybrid PV-thermal design, which enables producing both electrical
 422 energy and domestic hot water. Unarguably, PV panel cooling is beneficial both to its efficiency
 423 and lifespan (Sharma et al., 2018); however, a cooling system adds maintenance costs (Sato &
 424 Yamada, 2019), entails non-negligible water consumption or, in case that forced air cooling is
 425 implemented, subtracts output yield to the PV plant. Finally, the co-location of PV plants with
 426 green roofs can also aid cooling the PV panels (Jahanfar et al., 2020). For example, Cavadini
 427 and Cook (2021) found that the annual energy yield of PV panels on a green roof in Zurich,
 428 Switzerland, would be 1.8% higher than the same PV panels on a gravel roof.
 429
 430



431 *Figure 10.- Perspective image of the experimental and commercial areas with c-Si panels of the same model.*

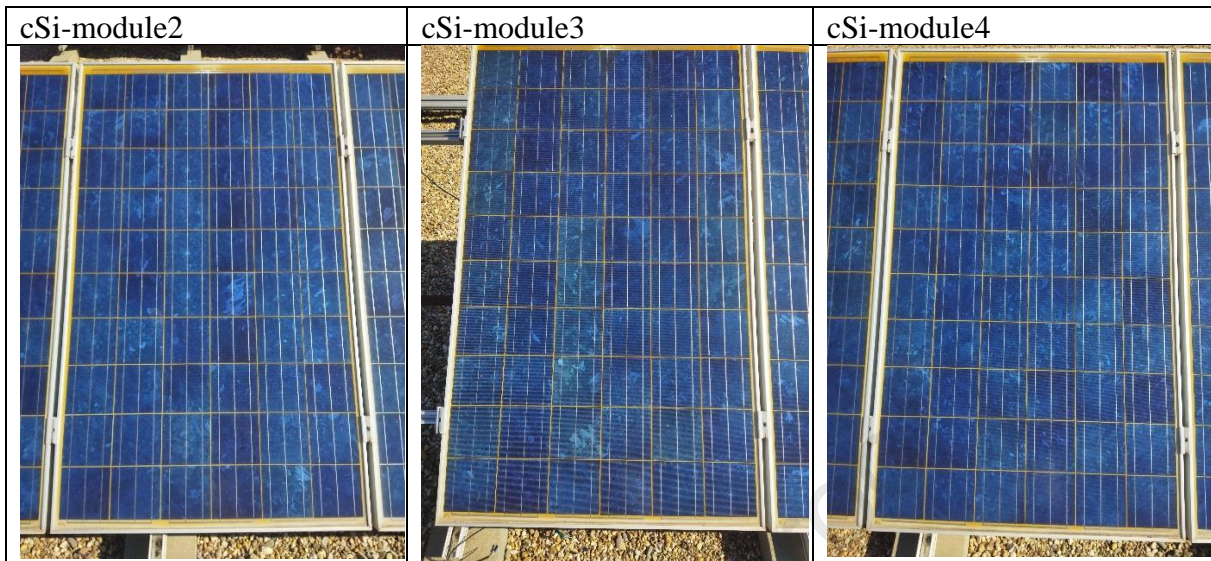
432



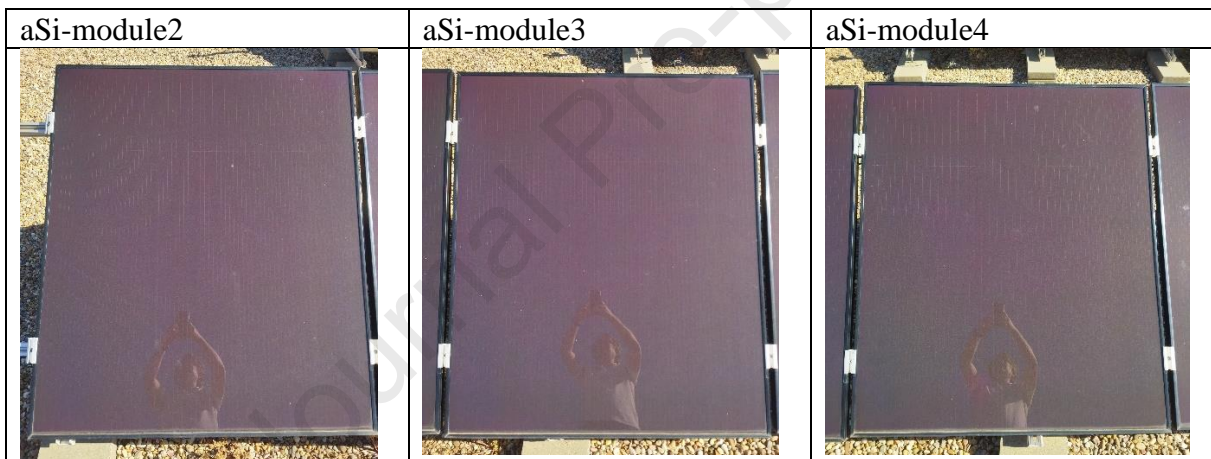
433 *Figure 11.- Close-up image of two of the CdTe PV modules with visual defects.*

434

435 The following figures show the current state after more than 10 years of operation, of the
 436 modules involved in the study as well as a view of the corresponding experimental part.
 437

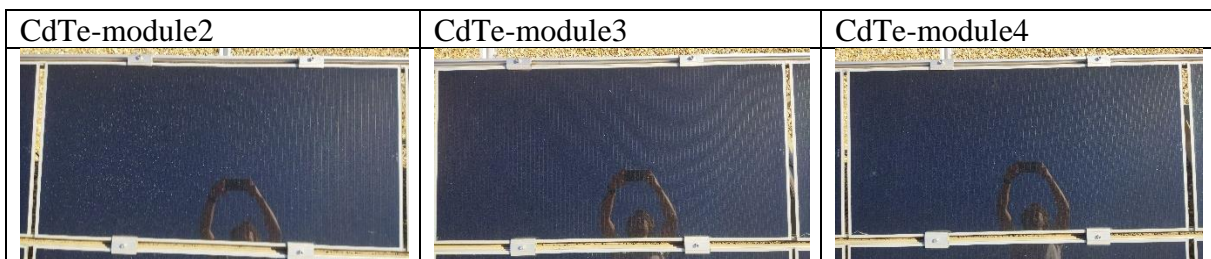


438 *Figure 12.- View of the three installed and working cSi modules used in for the analysis.*



439 *Figure 13.- View of the three installed and working aSi modules used in for the analysis.*

440
 441
 442
 443



444 *Figure 14.- View of the three installed and working CdTe modules used in for the analysis.*

445
 446 Kettle et al. (2022) summarized the specific degradation mechanisms of different PV
 447 technologies. For CdTe, they divided degradation mechanisms in two groups: Those related to
 448 the electrodes, and those related to the absorber. For the front electrode, they highlighted

449 potential induced degradation (PID), while for the rear electrode they mentioned copper
450 diffusion to front junction and molybdenum back contact oxidation. With regard to the
451 absorber, they pointed to migration of sodium from the panel soda-lime glass to the absorber or
452 CdTe-based cell. From the electrical point of view, ultimately copper diffusion provokes a
453 decrease in V_{oc} . Barbato et al. 2021, present a comprehensive review of the history, operation
454 and reliability of CdTe solar cells. Among the recent cases studies, they present the stress at
455 high temperature as one of the conditions that involve degradation, accounting for Cu and its
456 migration in crystal lattice as one of the relevant degradation processes.

457

458 In our case, PID should not be considered a plausible cause of degradation rate in the CdTe
459 panels, since these are frameless. Sodium migration from the panel glass cover should not be
460 an issue either, since our panels belong to a commercial generation that includes a barrier below
461 the glass. Contrarily, copper diffusion could play a role in the degradation rate observed, since
462 the Cdte technology of the panels installed, namely the Series 3 by the manufacturer First Solar,
463 did not yet include the countermeasures against copper diffusion of their recent siblings (Series
464 4 onwards by the same manufacturer). One of these countermeasures is a ZnTe back contact
465 (Scarpulla et al., 2023). This insight aligns with the broader findings on protective coatings
466 presented by Nakamura et al. (2023), and Kettle et al., who emphasized the versatility of
467 coatings in countering a range of degradation mechanisms. For instance, anti-reflective coatings
468 reduce surface reflectivity, improving light capture as noted by Scarpulla et al (2023).
469 Meanwhile, Nakamura et al. discussed hydrophobic coatings, which prevent moisture ingress,
470 a major factor in delamination and encapsulant degradation in humid environments. UV-
471 resistant layers further extends PV lifespans by protecting sensitive interfaces from
472 photodegradation. Scarpulla et al. described coatings that use chlorine or selenium to improve
473 passivation at grain boundaries in CdTe PV modules. The evidence is clear: protective coatings
474 significantly reduce degradation rates over time. Kettle et al reported annual degradation rates
475 ranging from 0.2% to 4% in CdTe and m-Si PV modules, highlighting the potential of coating
476 to stabilize performance.

477

478

479 5. Conclusions and future works

480

481 Experiments were carried out to analyse the effect of the course of time at plant half-lifetime
482 on the performance of three different PV technologies. The sample included 12 PV modules,
483 including emerging technologies like a-Si and CdTe.

484

485 The performance of three PV technologies under identical conditions over eleven years shows
486 some differences in their long-term stability and efficiency. All the modules analysed present,
487 an operation within the tolerances given by the manufacturer, and none of them show a power
488 drop of more than 1% per year.

489 - Crystalline silicon modules exhibit the lesser degradation, confirming their technological
490 maturity. These are monofacial and single junction multicrystalline panels.

491 - The amorphous silicon modules, in tandem or double junction a-Si:H-a-Si:H configuration,
492 after the initial drop in power due to stabilization, warned by the manufacturer, present stability
493 with an average power drop of 0.2%/year. Furthermore, under high temperature conditions, its
494 relative performance increases due to regeneration or thermal annealing.

495 - The case of cadmium telluride modules demonstrates a moderate degradation rate, being a
496 technology that, due to its efficiency and with the improvement in characteristics in the latter
497 years, would be one of the most promising technologies.

498

499 This real-world, comprehensive performance, degradation, and annealing analysis provides
500 valuable insights into the long-term performance and reliability of different PV technologies
501 under real-world operating conditions.

502
503 To continue obtaining valid data for the underlying of the degradation process,
504 electroluminescence images would be a valuable tool for the analysis of the cracks and broken
505 cells that is supposed that would appear with the pass of the years. Also thermographies would
506 help to detect the presence or absence of hot spots, that could be even related to the
507 electroluminescence analysis.

508 509 6. Acknowledgments

510 The authors acknowledge the research support to CIEMAT.

514 References

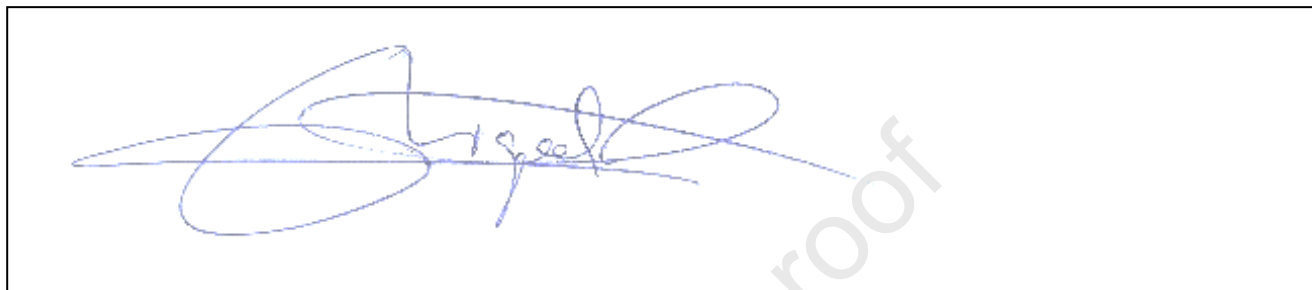
- 515
516 Barbato, Marco et al (2021). CdTe solar cells: technology, operation and reliability. *J. Phys. D: Appl. Phys.* 54: 333002
517
518 Berov et al. (2014). Outdoor degradation of thin film amorphous silicon based PV modules. *J. Phys.: Conf. Ser.*, 558: 012047.
519
520 Cavadini, G.B.; Cook, L.M. (2021). Green and cool roof choices integrated into rooftop solar energy modelling. *Applied Energy*, 296: 117082.
521
522 Dida, M.; et al. (2021). Experimental investigation of a passive cooling system for photovoltaic modules efficiency improvement in hot and arid regions. *Energy Conversion and Management*, 243: 114328.
523
524 Fraunhofer ISE. (2024). Photovoltaics report. Freiburg, 17 May 2024. Available at: www.ise.fraunhofer.de . Last accessed: June 2024.
525
526 Hamelmann et al. (2016). Light-induced degradation of thin film silicon solar cells. *J. Phys.: Conf. Ser.*, 682: 012002.
527
528 Ichikawa et al. (1990). A stable 10% solar cell with a-Si/a-Si double junction structure. IEEE Conference on Photovoltaic Specialists, 1475-1480. DOI: 10.1109/PVSC.1990.111854.
529
530 International Electrotechnical Commission. “Standard IEC 60904-9: Photovoltaic Devices. Part 9: Solar Simulator Performance Requirements”. IEC Central Office: Geneva, Switzerland, 2007.
531
532 Jahanfar, A.; et al. (2020). An experimental and modeling study of evapotranspiration from integrated green roof photovoltaic systems. *Ecological Engineering*, 152: 105767.
533
534 Kettle et al. (2022). Review of technology specific degradation in crystalline silicon, cadmium telluride, copper indium gallium selenide, dye sensitised, organic and perovskite solar cells in photovoltaic modules: Understanding how reliability improvements in mature technologies can enhance emerging technologies. *Prog. Photovolt. Res. Appl.*, 30: 1365-92.
535
536 Mateo et al. (2018). Analysis of initial stabilization of cell efficiency in amorphous silicon photovoltaic modules under real outdoor conditions. *Renewable Energy*, 120: 114-125.
537
538 McMahon T.J. (2004) Accelerated Testing and Failure of Thin-film PV Modules. *Prog. Photovolt: Res. Appl.* 2004; 12:235–248 (DOI: 10.1002/pip.526).
539
540 Ministerium of Industry of Spain. (2008). Royal Decree 1578/2008, of retribution of the activity of solar photovoltaic electric energy production. Official Bulletin (BOE) no. 234 of September 27th 2008.
541
542 Munoz et al. (2011). Influence of initial power stabilization over crystalline-Si photovoltaic modules maximum power. *Prog. Photovolt. Res. Appl.*, 19: 417-422.
543
544 Muñoz-García et al. (2021). Effects of the biggest snowfall of a century in Madrid, on the electricity production of portrait versus landscape layout solar panels. 38th EUPVSEC, 5CV.2.24, 1238-1240. DOI: 10.4229/EUPVSEC20212021-5CV.2.24.
545
546 Nakamura et al. (2023). Long-term examinations up to 20 years of performance ratio and degradation rate of different-type photovoltaic modules at central part of Japan. *Renewable Energy Focus*, 44: 98-105.
547
548 Pascual et al. (2021). Long-term degradation rate of crystalline silicon PV modules at commercial PV plants: An 82-MWp assessment over 10 years. *Prog. Photovolt. Res. Appl.*, 29: 1294-02.
549
550 Piliougine et al. (2022a). New model to study the outdoor degradation of thin-film PV modules. *Renewable Energy*, 193: 857-69.

- 551 Piliouguine et al. (2022b). Analysis of the degradation of amorphous silicon-based modules after 11 years of exposure by means
552 of IEC60891:2021 procedure 3. *Prog. Photovolt. Res. Appl.*, 30: 1176-1187.
- 553 Radue, D., Van Dyk, EE. (2010) A comparison of degradation in three amorphous silicon PV module technologies, *Solar*
554 *Energy Materials and Solar Cells*, Volume 94, Issue 3, 2010, Pages 617-622, <https://doi.org/10.1016/j.solmat.2009.12.009>.
- 555 REE, Red Eléctrica de España. (2024). Informe del Sistema eléctrico. Available at: [www.sistemaelectrico-ree.es/informe-del-](http://www.sistemaelectrico-ree.es/informe-del-sistema-electrico)
556 [sistema-electrico](http://www.sistemaelectrico-ree.es/informe-del-sistema-electrico)
- 557 Sato, D.; Yamada, N. (2019). Review of photovoltaic module cooling methods and performance evaluation of the radiative
558 cooling method. *Renewable and Sustainable Energy Reviews*, 104: 151-166.
- 559 Scarpulla et al. (2023). CdTe-based thin film photovoltaics: Recent advances, current challenges and future prospects. *Solar*
560 *Energy Materials & Solar Cells*, 255: 112289.
- 561 Sharma, R.; et al. (2018). Life span and overall performance enhancement of solar photovoltaic cell using water as coolant: A
562 recent review. *Materials Today: Proceedings*, 5: 18202-18210.
- 563 Staebler and Wronski (1997). Reversible conductivity changes in discharge-produced amorphous SI. *Applied Physics Letters*,
564 Vol. 31, No.4, 15 August 1977
- 565 Stuckelberger et al. (2017). Review: Progress in solar cells from hydrogenated amorphous silicon. *Renewable Sustainable*
566 *Energy Reviews*, 76: 1497-1523.
- 567 Wang et al. (2017). Seasonal performance comparison of three grid connected photovoltaic systems based on different
568 technologies operating under the same conditions. *Solar Energy*, 144: 798-807.
- 569 Wolf M., Rauschenbach H. (1963). Series Resistance effects on solar cells measurements. *Advanced Energy Conversion Vol*
570 *3*, pp. 445-479.

Declaration of interests

The authors declare that they have no known competing financial interests or personal relationships that could have appeared to influence the work reported in this paper.

The authors declare the following financial interests/personal relationships which may be considered as potential competing interests:



Journal Pre-proof